

Reservoir Characterization of the Middle Jurassic Lower Safa Member in the West Kanayes Fields, North Western Desert, Egypt.

Adel M. Salem ^{a,g}, Ali E. Abbas ^b, Ahmed A. Elnaggar ^b, Tamer M. Salem ^c, Mohamed A. Kassab ^d and Ahmed S. Attiya ^{e,*}

^a Department of Petroleum Engineering, Faculty of Petroleum and Mining Engineering, Suez University, Egypt.

^b Department of Geological and Geophysical Engineering, Faculty of Petroleum and Mining Engineering, Suez University, Egypt.

^d Department of Exploration, Khalda Petroleum Company, Cairo, Egypt.

^c Department of Exploration, Egyptian Petroleum Research Institute (EPRI), Cairo, Egypt.

^d Department of Exploration, Khalda Petroleum Company, Cairo, Egypt.

^e Department of Petroleum Engineering, Future University in Egypt (FUE), Cairo, Egypt.

*Corresponding author e-mail: aisa1@pme.suezuni.edu.eg

Abstract

Article Info

Received 21 Dec. 2025

Revised 22 Feb. 2025

Accepted 06 Apr. 2025

Keywords

"West Kanayes field; northwestern Desert; Lower Safa Member; Petrophysical parameters; hydrocarbon saturation"

The objective of this study is to evaluate the Lower Safa Member in the West Kanayes field, located in the north Western Desert of Egypt. This evaluation is based on qualitative and quantitative well-log data from five wells: WKAN D-1X, WKAN E-1X, WKAN F-1X, WKAN I-1X, and WKAN N-1X. The initial identification of potential reservoir zones was conducted by visually inspecting well log curves. Zones with favorable log responses such as low gamma ray readings, positive resistivity separation, and neutron-density separation indicative of sandstone were selected for further analysis. Key petrophysical parameters, including shale content, effective porosity, and water saturation, were computed using established equations. The results indicate that the WKAN D-1X well contains one promising interval characterized by the average effective porosity 7.5% and higher hydrocarbon saturation of average value of nearly 64% and the net pay thickness 3 ft. In contrast, the WKAN E-1X well contains one promising interval characterized by high effective porosity with averaging 8.1% and higher hydrocarbon saturation of average value 85% and the net pay thickness 3 ft. WKAN F-1X well identified one promising zone, with effective porosity 7.3% and the hydrocarbon saturation of average value 59.7% and the net pay thickness 4 ft. The WKAN I-1X well contains eight promising intervals characterized by high effective porosity with averaging 8.9% and higher hydrocarbon saturation of average value 66.6% and the net pay thickness 58 ft. Similarly, the WKAN N-1X well showed four zones with effective porosity 10.3% and the hydrocarbon saturation of average value 65.3% and the net pay thickness 44 ft. Through our study, we found that the Lower Safa Member composed of a mixture of siltstone, sandstone, shale, and occasional limestone and coal streaks, according to lithological identification. Overall, the Lower Safa Member exhibits potential hydrocarbon-bearing zones with varying degrees of reservoir quality, influenced by shale content and porosity levels. This evaluation provides a foundation for further exploration and development in the West Kanayes fields.

1- Introduction

The northern Western Desert encompasses seven basins: Matruh, Shushan, Dahab, Natrun, Ghazalat, Gindi, and Abu Gharadig basins. These basins have attracted numerous oil companies for hydrocarbon exploration. The hydrocarbon exploration in these sedimentary basins is controlled by a complex geological history and a variety of depositional environments (El Gazzar et al., 2016; Assal et al., 2021; Sarhan, 2019). An area of the Northwestern Desert of Egypt occupies an approximately 250.000 Km²

from the total area of Egypt. It is almost completely covered by Tertiary and Quaternary sedimentary rocks, which forms a major part of the unstable (mobile) shelf of Egypt Said, R. (1962). The study area in Matruh Basin is in the Northern Western Desert of Egypt and a part of Khalda concession. The area under study occupying an area is approximately 12 km². It lies between latitudes 27° 54' 00" - 27° 34' 00" E and latitudes 30° 52' 00" - 30° 38' 00" N Figure (1). The source rocks in the Middle Jurassic Lower Safa Member are generally rich and mature and were related to Type-III kerogen that capable of generating mainly gas with minor oil Attiya et al. (2022).

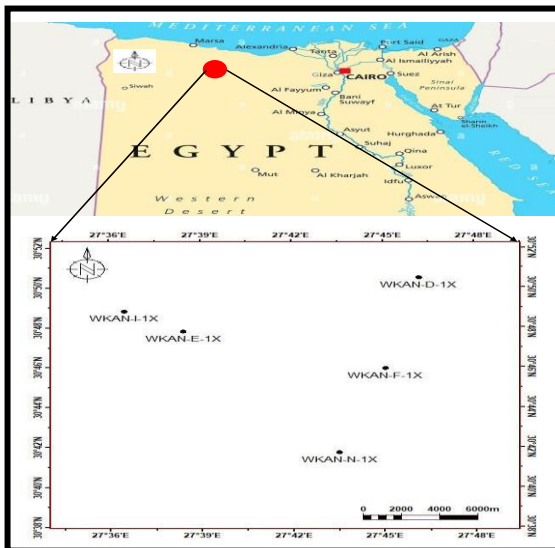


Figure 1 Location map of the studied wells in the West Kanayes concession, Northern Western Desert, Egypt.

There are many oil fields in the northern region of the western desert that are currently producing from thin, spaced intervals inside the thick section of Alam El Bueib, Hagra et al. (1992). The northern basins of the Jurassic-Cretaceous sands, especially the Matruh and Shushan basins, produce the majority of the oil used in the Western Desert Metwalli (2004).

The reservoir parameters such as porosity, water saturation, and shale volume can be identified by the interpretation of well logging data, these data are performed using the available software and offset well parameters (Schlumberger, 1984 & 1974; Kassab et al, 2020).

The analysis and associated computations were carried out using various electric Line Logging suites (Gamma Ray, Resistivity, Density, Neutron) for five wells: W KAN D-1X, W KAN E-1X, W KAN F-1X, W KAN I-1X, and W KAN N-1X. The most essential Petrophysical characteristics such as Shale Volume, Effective Porosity and Fluid Saturation, are inferred in order to characterize the possible reservoirs.

2- Geologic Setting

The Matruh Basin lithostratigraphy is composed of rock units ranging from the Precambrian to recent geologic time EGPC (1992) Figure (2). Fawzy and Dahi (1992), Early Cambrian to Late Permian Paleozoic sediments make up its unconformably overlying Precambrian basement, which is in turn unconformably covered with Jurassic deposits (Masajid and Khatatba, Eghei formations) and younger deposits. Thick Neocomian-Albian marine sediments that are split within the Shaltut, Betty and Alamein formations were deposited on continental clastics during the Early Cretaceous. The Kharita (clastics) and Dahab (mostly shale) formations lie on top of these rock units. On the other hand, the fine non-Clastic and Clastic deposits from deep marine deposits at the upper of the Chalk Limestone are made up of coarse clastics from a Shallow Marine environment at the foot of the Turonian and

Late Cenomanian sediments Soliman and Elbadry, (1980). There are seven members in the Abu Roash formation: A, B, C, D, E, F, and G. The members A, C, E, and G are mainly made up of clastics, whereas the members B, D, and F are mainly made up of Carbonates Schlumberger, (1995).

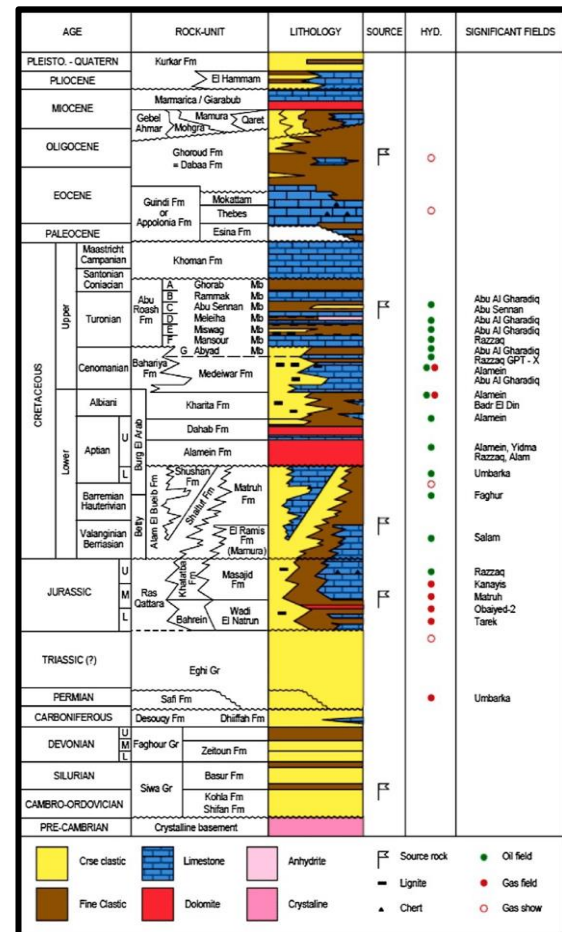


Figure 2 Generalized stratigraphic column of the north Western Desert, after (Schlumberger, 1995).

3- Materials and Methods

Five wells (W KAN D-1X, W KAN E-1X, W KAN F-1X, W KAN I-1X and W KAN N-1X). containing clastic reservoir rocks from the Middle Jurassic Lower Safa Member were analyzed & their hydrocarbon potential evaluated for this study. The LAS files containing the open-hole log data for the wells under investigation were gathered and processed into digital form.

The analysis, which has been carried out for different well logs (Gamma Ray, Neutron, Density, Sonic, Resistivity, etc.), was interpreted to evaluate the hydrocarbon potentiality of Lower Safa reservoir and to determine the thickness and depth of gas, oil, or water zones within the reservoir.

The analysis carried out by using Interactive Petrophysics (IP, v4.3) Schlumberger software, then interpreted to identify the depth and thickness of gas, oil, or water zones within the reservoir and determine the hydrocarbon potentiality of Lower Safa Reservoir.

Schlumberger (1974), The following equation can be used to get the effective porosity (Φ_e):

$$\Phi_e = \Phi_D - (\Phi_{D_{sh}} \times V_{sh}) \quad (1)$$

Where;

$$\Phi_D = (\rho_{b_{ma}} - \rho_{b_{log}}) / (\rho_{b_{ma}} - \rho_{b_f}) \quad (2)$$

$$\Phi_{D_{sh}} = (\rho_{b_{ma}} - \rho_{b_{sh}}) / (\rho_{b_{ma}} - \rho_{b_f}), \text{ and} \quad (3)$$

Φ_e = The effective porosity, fraction

$\rho_{b_{sh}}$ = The density of shale bed (gm/cc).

Φ_D = The density derived porosity,

$\rho_{b_{ma}}$ = The density of rock matrix (gm/cc),

$\rho_{b_{log}}$ = The density log reading for each interval (gm/cc), and ρ_{b_f} = The density of mud fluid in gm/cc

V_{sh} = Shale volume, fraction.

The amount of shale content (V_{sh}) in a reservoir is expressed as the wet shale volume per unit reservoir volume. Determining a reservoir's shale content is important because shale concentration has a big influence on log interpretation, which in turn influences reserve estimation and hydrocarbon production. **Asquith (1982)**, The clay minerals influence the permeability, water saturation, and porosity of reservoirs. The composition of the shale can be determined by utilizing a variety of petrophysical measurements, including gamma and neutron porosity.

$$V_{sh} = 0.33 (2^{(2 \cdot I_{GR})} - 1) \quad (4)$$

$$I_{GR} = (GR_{log} - GR_{cl}) / (GR_{sh} - GR_{cl}) \quad (5)$$

Where;

I_{GR} = Gamma ray index,

GR_{log} = Reading of Gamma ray log,

GR_{sh} = shale bed of Gamma ray, and

GR_{cl} = clean interval of Gamma ray.

Archie (1942), The basic method used for all water saturation estimation is Archie's equation. Water saturation (S_w) can often be determined using porosity and resistivity logs.

$$S_w^n = (F \times R_w) / R_t \quad (6)$$

Where;

R_w = Resistivity of formation water,

R_t = Resistivity reading in uninvaded zone,

S_w = Water saturation in uninvaded zone,

n = Saturation exponent, and

F = Formation resistivity factor which depends on the structure of the formation and has good relation with porosity.

$$F = a / \phi^m \quad (7)$$

Where, (m) and (a) are constant determined from local experience ($a=1$ & $m=2$).

All wells lithology and Lower Safa Member components have been studied applying logging crossplots, which included Neutron - Density Crossplots and M - N Cross plots. The Cross-plot points would be shifted to the downright or right from the baseline of pure sand due to the increase in shale content.

The most essential petrophysical characteristics, such as fluid saturation (water and hydrocarbons), shale volume, and porosity (total and effective), are inferred to characterize the possible reservoirs. Table (1) illustrates the available of well logging data for five wells in the West Kanayes field.

Table (1): Well logging data.

| No | Well Name | From (ft) | To (ft) | Logging |
|----|------------|-----------|---------|--|
| 1 | W KAN D-1X | 2800 | 15663 | LLD-LLS-CALI-SP-RHOM-APLC-DTCO-HSGR |
| 2 | W KAN E-1X | 200 | 14737 | RLA5-RLA3-RXOZ-HCAL-SP-RHOZ-APLC-DTCO-HSGR |
| 3 | W KAN F-1X | 9050 | 14167 | RLA5-RLA3-RXOZ-CAL-SP-RHOZ-APLC-DTCO-GR |
| 4 | W KAN I-1X | 200 | 15427 | LLD-LLS-CALI-SP-RHOM-APLC-DTCO-HSGR |
| 5 | W KAN N-1X | 200 | 15300 | RLA5-RLA3-RXOZ-CAL-SP-RHOZ-APLC-DTCO-GR |

4- RESULTS AND DISCUSSION

4.1 Petrophysical Evaluation

In the five wells that were chosen, a set of well logs has been run. WKAN D-1X, WKAN E-1X, WKAN F-1X, WKAN I-1X, and WKAN N-1X are the names of these wells. Gamma Ray, Resistivity, Density and Neutron logs made up the minimal suite of logs, all logs data are available in digital format.

4.1.1 Lithological interpretation using cross-plots

There are several ways to determine lithology. It's apparent in the composite log. The other technique for determining lithology from logs is to utilize crossplots. The cross-plot combinations under discussion are covered in Dresser Atlas (1979), Schlumberger (1974), and Poupon et al. (1970). M - N and Neutron - Density crossplots were the types of crossplots used in the present study. Shale influence is seen in the cross plot, where points typically fall into the southeast quadrant **Poupon et al. (1970)**.

4.1.1.1 Neutron - Density Crossplots

The Dia-porosity cross-plots is common in well log analysis and quick look interpretation to draw crossplots against different log driven parameters in order to identify the lithology and porosity in the formation. The Neutron-density cross-plots is considered the most widely used porosity log combination **Emad et al. (2021)**. Below is a description of the Density - Neutron crossplots that were created for the Middle Jurassic reservoirs:

The Density - Neutron crossplot of the Lower Safa reservoir Figure (3) reflects that porosity ranges from 7.3 to 10.3%, where the most points are scattered on and very close to sandstone line, while the rest points are plotted between sandstone and limestone. This indicates the presence of sandstone reservoir with some limestone streaks. Some points scattered toward dolomite line are attributed to dolomitic cement. The effect of gas is observed where some points are shifted upward above the sandstone line.

4.1.1.2 M - N Crossplots

The use of M - N Crossplots, which indicate the types of lithology, facilitates the understanding of minerals using density, Neutron and acoustic logs Bruke et al. (1969) introduced this plot for the first time. In this study, the sonic log data are available in five wells only. The **M** and **N** can be determined by using the following equations:

$$M = (\Delta t_f - \Delta t) / (\rho_b - \rho_{bf}) \times 0.01 \quad (8)$$

$$N = (\phi N_f - \phi N) / (\rho_b - \rho_{bf}) \quad (9)$$

Where;

Δt_f = Interval transit time of the mud fluid,

Δt = Sonic log reading,

ρ_b = Density log reading,

ρ_{bf} = Density of mud fluid,

ϕN_f = Neutron of mud fluid, and

ϕN = Neutron log reading.

The M - N cross plot of the Lower Safa reservoir shown in Figure (4). Many of the points are scattered between sandstone and limestone points but tend to be near to sandstone point more than limestone one. This indicates that there is a reservoir of sandstone with some streaks of limestone. Due to shale effect some points are scattered downwards and near the dolomite region. However, the effect of secondary porosity appears in shifting of some points upwards. Also, some points scattered in the upright corner, this indicates that the effect of gas.

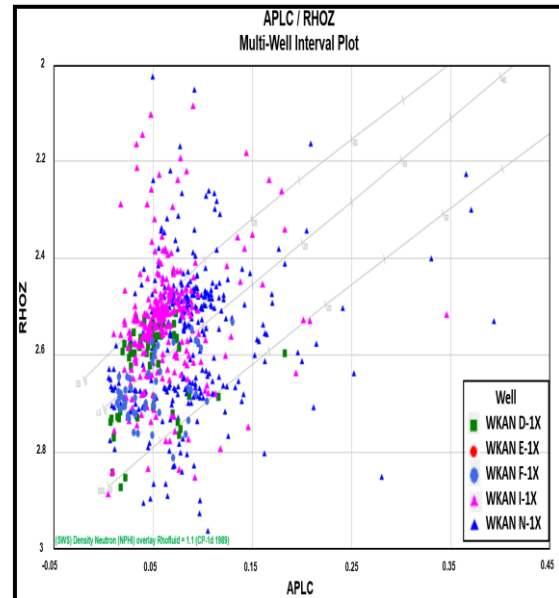


Figure 3 Neutron - Density crossplot of the Lower Safa Reservoir.

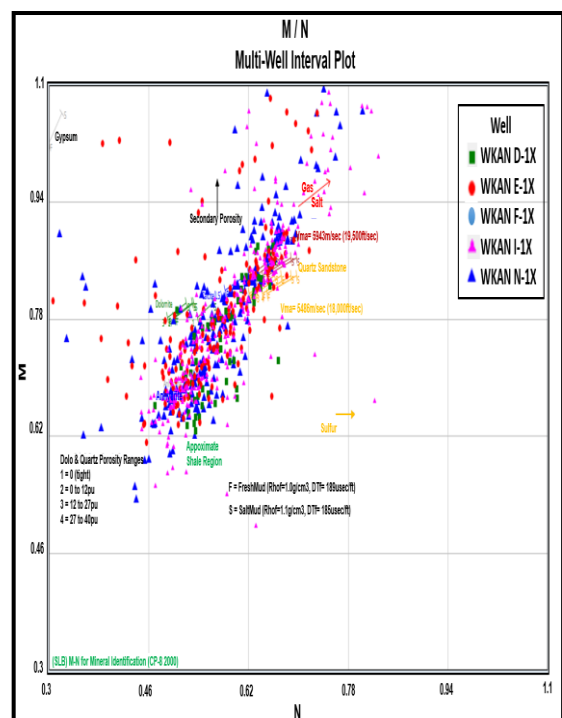


Figure 4 M - N crossplot of the Lower Safa Reservoir.

4.1.2 Evaluation of Hydrocarbon Potentiality

The interpretation of hydrocarbon potentialities takes place by the evaluation of the petrophysical parameters of the study formations Table (2). This interpretation was estimated by the vertical and horizontal distribution of the petrophysical results.

4.1.2.1 Vertical distribution of hydrocarbon occurrences

The formation analysis is done using this cross plot, which shows the vertical distribution of fluids, porosity (both total and effective porosity), and rocks (lithology). In WKAN D -1X well, Figure (5) represents that the vertical analysis of Lower Safa reservoir, extends from 14850 to 15146 feet. The reservoir thickness 296 feet. The rock units consist mainly of siltstone as a major lithology intercalated with appearing layers of sandstone, shale and Limestone. The average effective porosity 7.5%. The fluid analysis indicates that, the hydrocarbon saturation 64%. The net pays thickness 3 feet.

The In WKAN E-1X well, Figure (6) represents that, the vertical analysis of Lower Safa reservoir, extends from 13736 to 14738 feet. The reservoir thickness 1002 feet. The rock units consist mainly of siltstone and shale intercalated with sandstone, Limestone and some streaks of coal. The average effective porosity 8.1%. The fluid analysis indicates that, the hydrocarbon saturation 85%. The net pay thickness 3 feet. The average movable hydrocarbon is 53.1%, whereas the residual hydrocarbon 31.6%.

In WKAN F-1X well, Figure (7) represents that, the vertical analysis of Lower Safa reservoir, extends from 13595 to 14167 feet. The reservoir thickness 572 feet. The lithologies consist mainly of siltstone and shale are intercalated with sandstone, Limestone and some streaks of coal. The average effective porosity is 7.3%. The net pay thickness 4 feet. The average values of the movable hydrocarbon 43.1%, whereas the residual hydrocarbon 16.6%.

In WKAN I-1X well, Figure (8) shows that, the vertical analysis of Lower Safa reservoir, extends from 13785 to 15428 feet. The reservoir thickness is 1643 feet. The lithologies consist mainly of sandstone and are intercalated with siltstone, shale and some streaks of coal. The average effective porosity 8.9%. The fluid analysis shows that the hydrocarbon saturations are restricted in the upper part of the formation to reach 66.6% with net pay thickness 58 ft. The average movable hydrocarbons 21.6%, while the residual hydrocarbons reached 45%.

In WKAN N-1X well, Figure (9) shows that, the vertical analysis of Lower Safa reservoir, extends from 13727 to 15300 feet. The reservoir thickness 1573 feet. The lithologies consist mainly of sandstone and are intercalated with siltstone, shale and some streaks of coal. The average effective porosity 10.3%. The fluid analysis indicates that hydrocarbon saturation 65.3%. The net pay thickness 44 ft. The average movable hydrocarbon 39.1%, where the average residual hydrocarbon value is 26.2%.

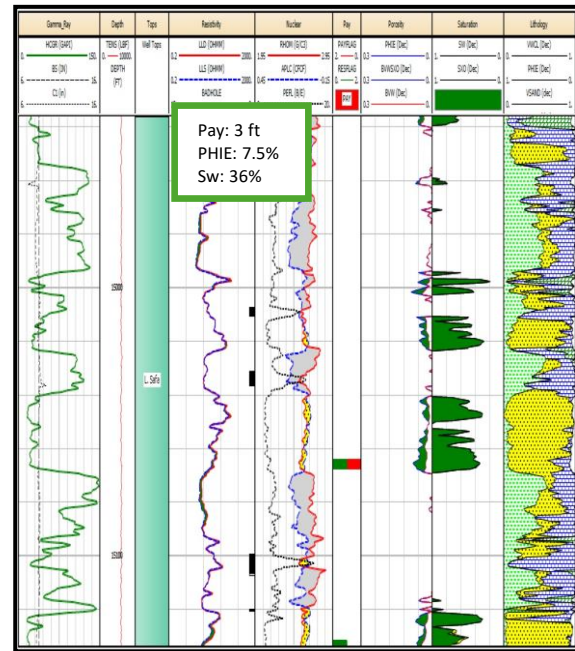


Figure 5 Litho-Saturation crossplot of Lower Safa Reservoir in WKAN D-1X well.

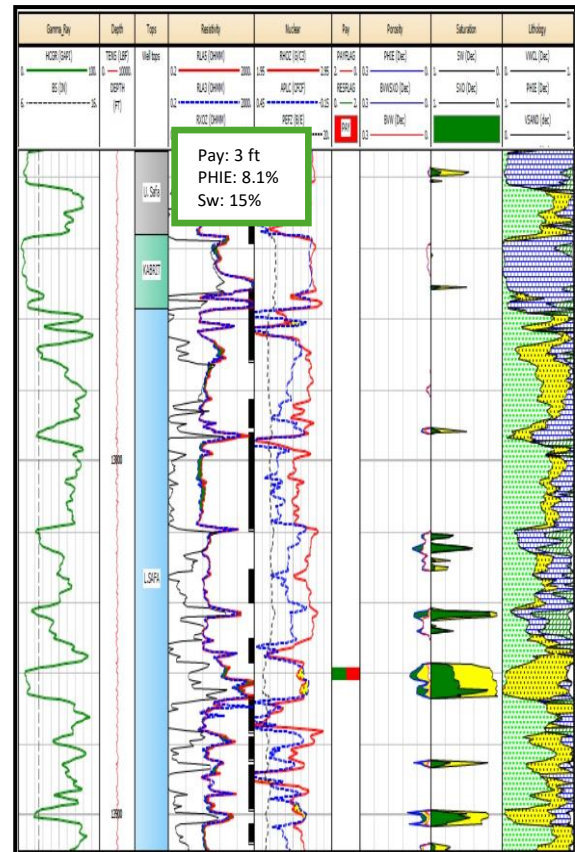


Figure 6 Litho-Saturation crossplot of Lower Safa Reservoir in WKAN E-1X well.

Table (2): The petrophysical analysis of the studied wells for Lower Safa reservoir.

| Petrophysical parameters | Well name / Reservoir name | | | | |
|--|----------------------------|-----------|-----------|-----------|-----------|
| | WKAN D-1X | WKAN E-1X | WKAN F-1X | WKAN I-1X | WKAN N-1X |
| | Lower Safa Reservoirs | | | | |
| Total Thickness [ft] | 296 | 1002 | 572 | 1643 | 1573 |
| Total Porosity [%] | 7.8 | 8.4 | 10 | 9.1 | 11.1 |
| Effective Porosity [%] | 7.5 | 8.1 | 7.3 | 8.9 | 10.3 |
| Shale Volume [Vsh%] | 6 | 5.2 | 17.1 | 3.5 | 6.8 |
| Gross Sand [ft] | 138.5 | 238 | 57 | 641 | 412 |
| Net Pay [ft] | 3 | 3 | 4 | 58 | 44 |
| Net / Gross [N / G, %] | 2.2 | 1.3 | 7 | 9 | 10.7 |
| Flushed Zone Saturation [Sxo, %] | 36.3 | 68.4 | 83.4 | 55 | 73.8 |
| Water Saturation [Sw, %] | 36 | 15 | 40.3 | 33.4 | 34.7 |
| Hydrocarbon Saturation [Sh, %] | 64 | 85 | 59.7 | 66.6 | 65.3 |
| Residual Hydrocarbon Saturation [Shr, %] | 63.7 | 31.6 | 16.6 | 45 | 26.2 |
| Movable Hydrocarbon Saturation [Shm, %] | 0.3 | 53.4 | 43.1 | 21.6 | 39.1 |

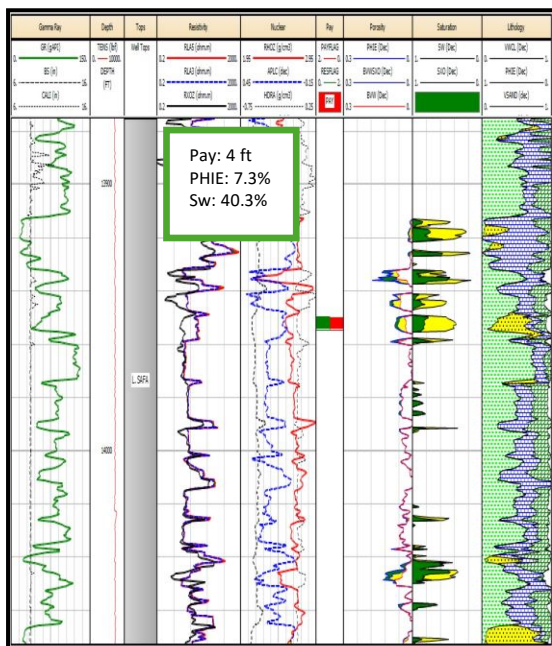


Figure 7 Litho-Saturation crossplot of Lower Safa Reservoir in WKAN F-1X well

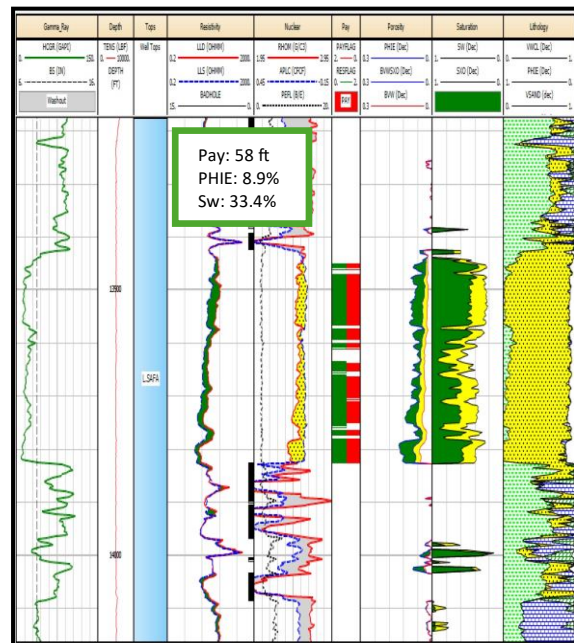


Figure 8 Litho-Saturation crossplot of Lower Safa Reservoir in WKAN I-1X well.

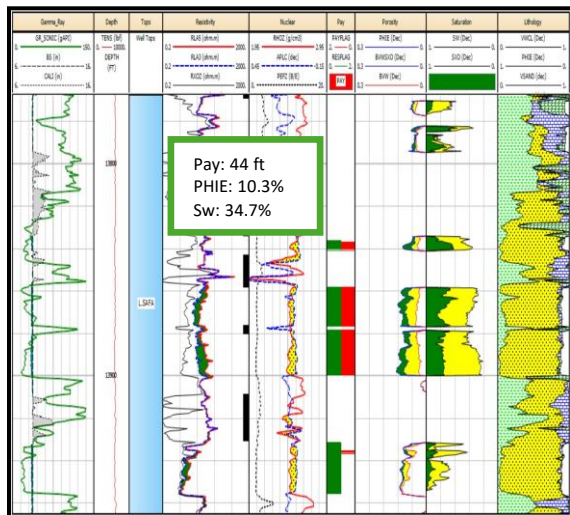


Figure 9 Litho-Saturation crossplot of Lower Safa Reservoir in WKAN N-1X well.

4.1.2.2 Horizontal distribution of hydrocarbon occurrences

The process of creating isoparametric maps of the research region allows for the horizontal distribution of petrophysical characteristics. The following mapping includes the Lower Safa Reservoir for the five wells in the research area (WKAN D-1X, WKAN E-1X, WKAN F-1X, WKAN I-1X, and WKAN N-1X).

The total thickness distribution map of the Lower Safa Reservoir illustrated in Figure (10). The total thickness rises in the west and southwest directions of the study area, with maximum value 1643 feet in WKAN I-1X well and declines towards the northeast direction of the study area, with minimum value 296 feet in WKAN D-1X well.

The total porosity distribution map of the Lower Safa Reservoir Figure (11) shows remarkable increase in the total porosity toward south portion direction of the study area and gradually decreases from the middle portion to the northeast direction, with maximum value of 11.1% at WKAN N-1X well, and the minimum of 7.8% at WKAN D-1X well.

The effective porosity in the Lower Safa Reservoir increases toward south direction and extend to the southwest direction, where it reaches 10.3% at WKAN N-1X well, and decreases toward the east direction to reach 7.3% at WKAN F-1X well Figure (12).

The water saturation in the Lower Safa Reservoir increases toward the east direction and extends to the southeast direction, with maximum value of 40.3% in WKAN F-1X well, and decreases in the central portion of the area, with minimum value of 15% at WKAN E-1X well Figure (13).

The shale volume in the Lower Safa Reservoir increases toward the east direction with the highest value of 17.1% in WKAN F-1X well, and decreases in the western portion of the area, with lowest value of 3.5% in WKAN I-1X well Figure (14).

The gross sand map of the Lower Safa Reservoir Figure (15) shows a marked increase in the west direction with the maximum value of 641 ft. in WKAN I-

1X well, and it decreases in the west direction to reach the minimum value 57 ft. in WKAN F-1X well.

The net pay in the Lower Safa Reservoir increases almost in the western portion of the research area and extends to southwest directions with highest value 58 feet in WKAN I-1X well and decreases from the middle portion to the northeast directions of the research area, with lowest value 3 feet in WKAN E-1X well Figure (16).

The hydrocarbon saturation map in the Lower Safa Reservoir Figure (17) increases at the middle portion of the area with highest value 85% at WKAN E-1X well and decreases laterally toward the eastern portion of the study area, with lowest value 59.7% in WKAN F-1X well.

The residual hydrocarbon saturation in the Lower Safa Reservoir Figure (18) increases at the northern portion of the area with a maximum value of 63.7% at WKAN D-1X well. This value decreases in the southeastern portion of the area with a minimum value of 16.6% at WKAN F-1X well.

The movable hydrocarbon saturation in the Lower Safa Reservoir Figure (19) increases from the middle portion of the research area to the southeast direction and extends to south direction, with maximum value of 53.4% at WKAN E-1X well, and decreases toward the northern portion of the study area with minimum value of 0.3% at WKAN D-1X well.

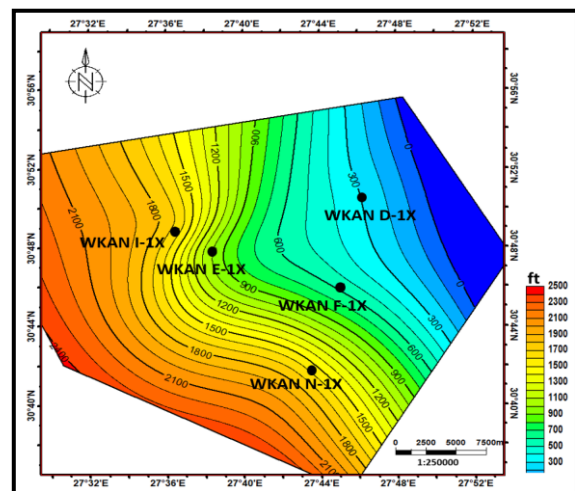


Figure 10 Total thickness map of the Lower Safa reservoir.

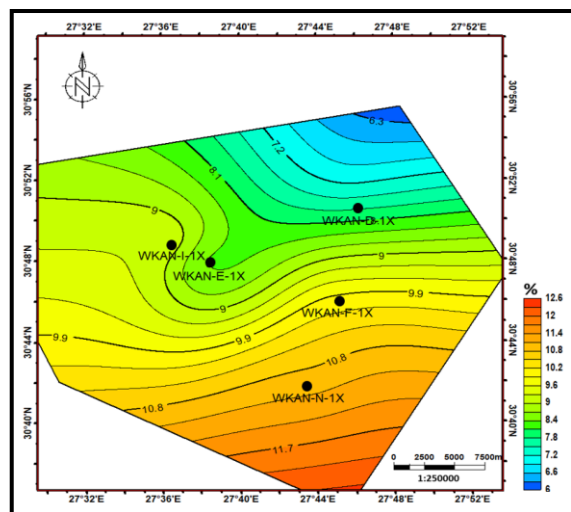


Figure 11 Total porosity map of the Lower Safa reservoir.

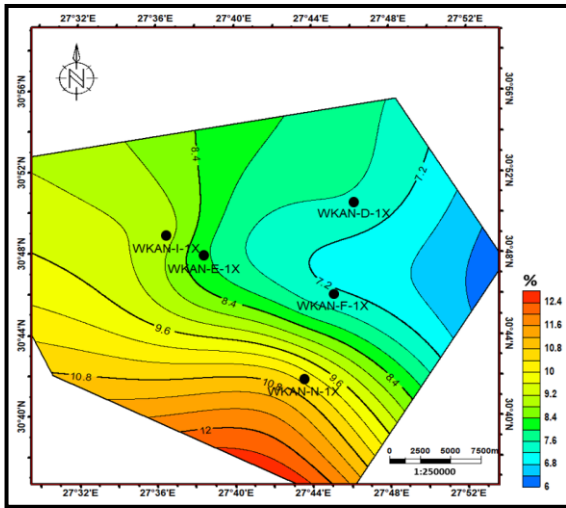


Figure 12 Effective porosity map of the Lower Safa reservoir.

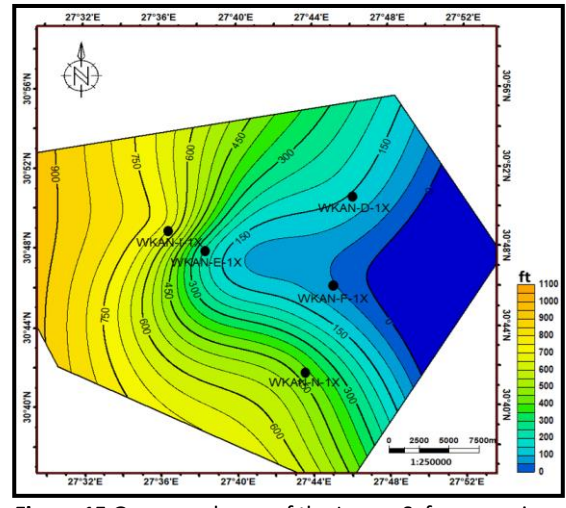


Figure 15 Gross sand map of the Lower Safa reservoir.

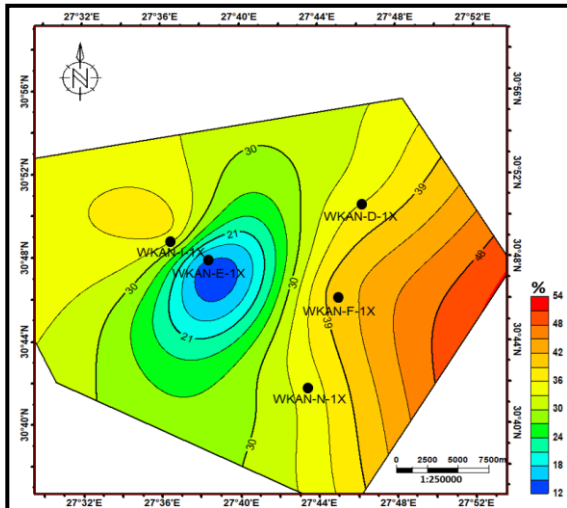


Figure 13 Water saturation map of the Lower Safa reservoir.

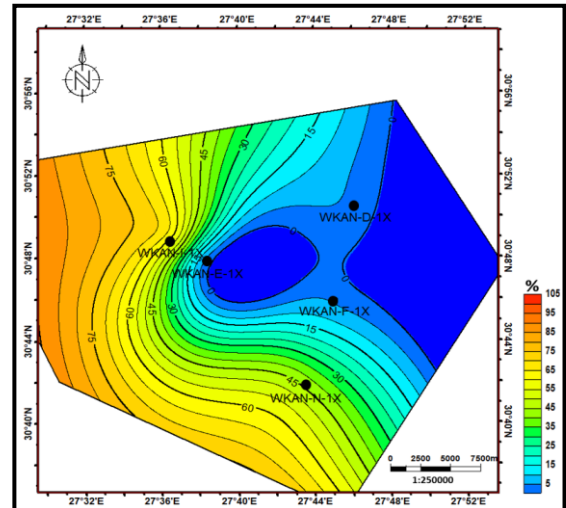


Figure 16 Net pay thickness map of the Lower Safa reservoir.

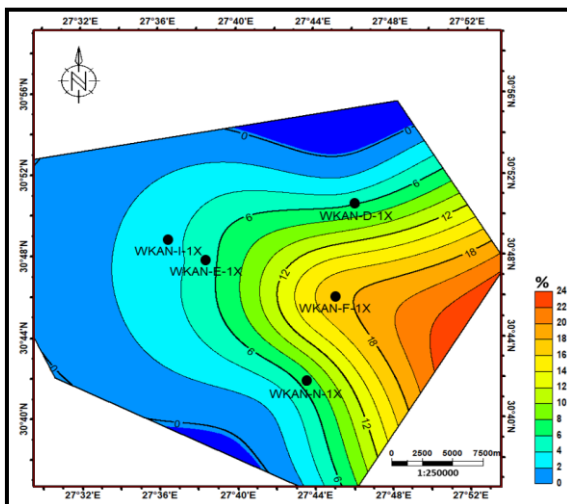


Figure 14 Shale volume map of the Lower Safa reservoir.

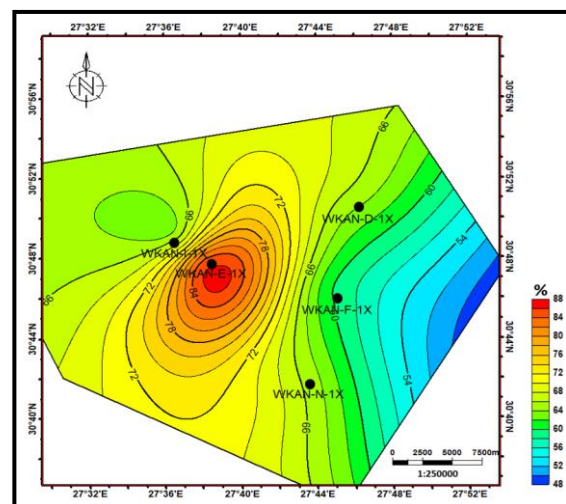


Figure 17 Hydrocarbon saturation map of the Lower Safa reservoir.

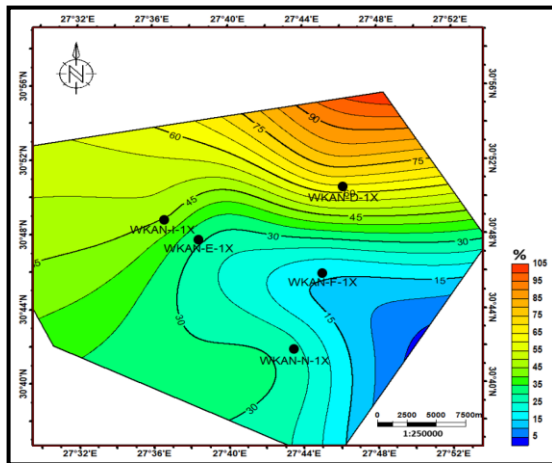


Figure 18 Residual hydrocarbon saturation map of the Lower Safa reservoir.

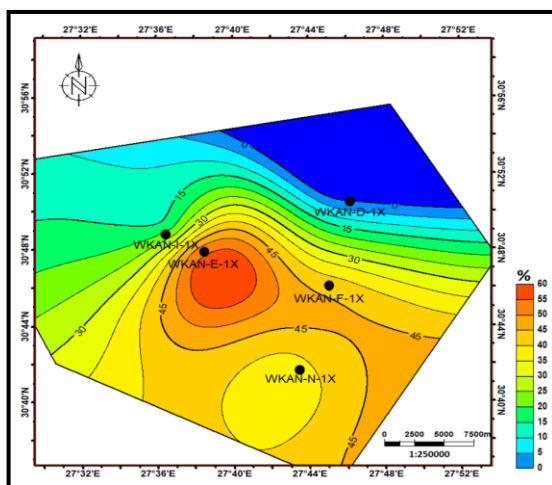


Figure 19 Movable hydrocarbon saturation map of the Lower Safa reservoir.

4.1.3 Isopach Maps:

An important isopach map is the interpretation, which includes restoration of the original depositional edge of the stratigraphic unit. In some instances, the present day zero isopach lines may represent the shore of the ancient sea which deposited at that time Krumbein and Sloss (1963). The isopach map is constructed for the Lower Safa reservoir to evaluate the variation in the thickness of one reservoir Table (3).

The Isopach map shows variations in thickness of Lower Safa Member through the different studied wells Figure (20). The thickness reaches the greatest value of about 1643 feet at WKAN I-1X well and the lowest value of about 296 ft at WKAN D-1X well. Furthermore, the increasing in thickness towards the northwest, west and southwest directions indicates a deep basin of deposition at that time and the wide contour in the northeastern part may indicate a gentle gradient of deposition than in the other parts.

4.1.4 Facies Maps:

The areal variation of the various stratigraphic units is displayed on facies maps. These maps are created for several purposes, including the interpretation of

environmental conditions, the reconstruction of geological history, the assessment of the tectonic configuration of the present, and/or other commercial uses Krumbein (1952).

The total thickness of each stratigraphic division, as well as the lithology of each rock type, individual or assembled as a member, percentage of sand / shale and clastic / non clastic percentage are calculated using Krumbein and Sloss (1963).

Technique as follows:

$$\text{Clastic percentage} = \frac{\text{Thickness of clastic in the unit}}{\text{Total Thickness of the unit}} \times 100$$

$$\text{Sand / Shale ratio} = \frac{\text{Sand} + \text{Sandstone} + \text{Conglomerate}}{\text{Shale} + \text{siltstone}}$$

Many isolith maps have been prepared as thickness maps, to avoid confusion in the use of the term, it described as thickness isolith map or for example, simply as a "sandstone thickness map". Table (4) showing the data of facies maps were constructed for Lower Safa reservoir.

Lithologically, the sandstone, siltstone, and shale found in the Lower Safa reservoir deposits, as well as occasional limestone streaks, represent fluvio-marine to shallow marine facies.

To understand the environmental circumstances surrounding the sediment deposit and to provide information on the region's geological past, isolith maps were created for the Lower Safa. These maps display variations in the thickness of a single rock type.

Sandstone isolith map of Lower Safa Member Figure (21), sandstone thickness Table (4) increases toward the west direction and extends to the south direction of the research area, with greatest thickness of about 641 feet in WKAN I-1X well, and the least thickness 57 feet is recorded at WKAN F-1X well.

Siltstone isolith map of Lower Safa Member, siltstone thickness Table (4) increases toward the west and southwest directions and extend to the west direction of the area Figure (22), with highest thickness value of 594 feet, at WKAN I-1X well, and the siltstone thickness decreases from middle area to east and northeast directions of the research area, with lowest thickness value of 110.5 feet, at WKAN F-1X well.

Shale isolith map of Lower Safa Member, shale thickness Table (4) increases from middle portion to southwest, south and west directions of the research area Figure (23), with highest thickness value of 313 feet, at WKAN E-1X well, and the Shale thickness decreases towards the northeast direction, with lowest thickness value of 2.5 feet, at WKAN D-1X well.

Limestone isolith map of Lower Safa Member, limestone thickness Table (4) increases from the middle portion to the southwest direction and extend to the west and south directions of the research area Figure (24), with highest thickness value of 163 feet, at WKAN N-1X well, and the limestone thickness decreases towards the northeast direction, with lowest thickness value of 25 feet, at WKAN D-1X well.

The Lithofacies distribution map of Lower Safa Member shows that the triangle facies map is characterized by clastic facies. The argillaceous sandstone facies are changing to sandy shale Figure (25). These facies reflect a continental to a fluvio-deltaic environment.

Table (3): The total thickness of Lower Safa reservoir.

| Well | Rock Unit |
|-----------|------------|
| | Lower Safa |
| WKAN D-1X | 296 |
| WKAN E-1X | 1002 |
| WKAN F-1X | 572 |
| WKAN I-1X | 1643 |
| WKAN N-1X | 1573 |

Table (4): Data for facies maps of Lower Safa reservoir in studied wells.

| Well | Thickness ft | SST ft | SLT ft | SH ft | LST ft | clastic % | non clastic % | SST/SH ratio |
|-----------|--------------|--------|--------|-------|--------|-----------|---------------|--------------|
| WKAN D-1X | 296 | 138 | 129 | 2.5 | 25 | 91.5 | 8.5 | 1.05 |
| WKAN E-1X | 1002 | 238 | 215 | 313 | 162 | 76.5 | 16.5 | 0.45 |
| WKAN F-1X | 572 | 57 | 110 | 198 | 102 | 77.8 | 21.8 | 0.19 |
| WKAN I-1X | 1643 | 641 | 594 | 217 | 129 | 91.8 | 8.2 | 0.79 |
| WKAN N-1X | 1573 | 412 | 484 | 308 | 163 | 88.1 | 11.9 | 0.52 |

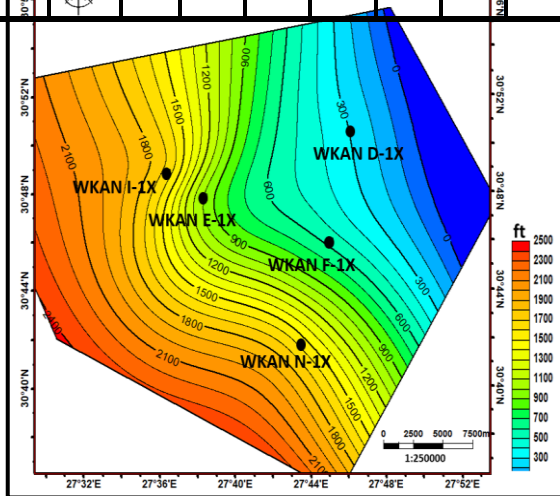


Figure 20 Isopach map of the Lower Safa reservoir.

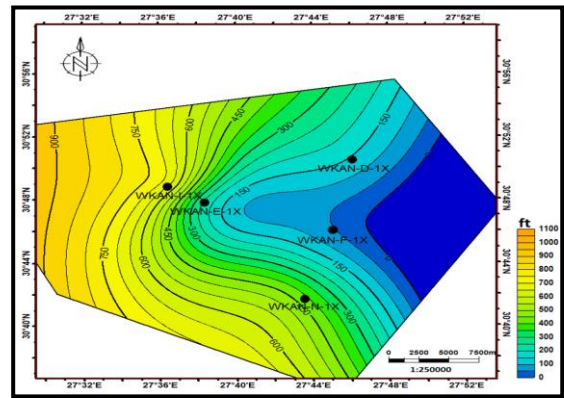


Figure 21 Sandstone isolith map of the Lower Safa reservoir.

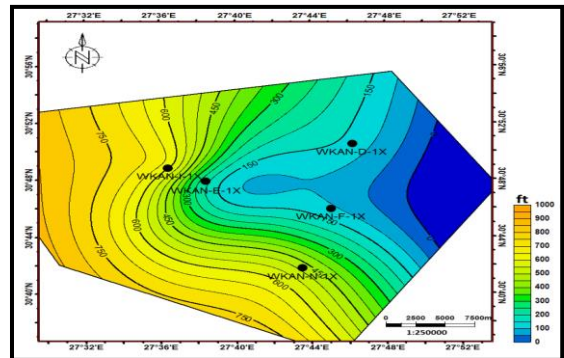


Figure 22 Siltstone isolith map of the Lower Safa reservoir.

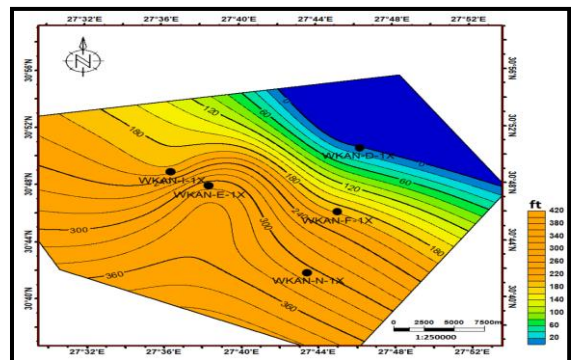


Figure 23 Shale isolith map of the Lower Safa reservoir.

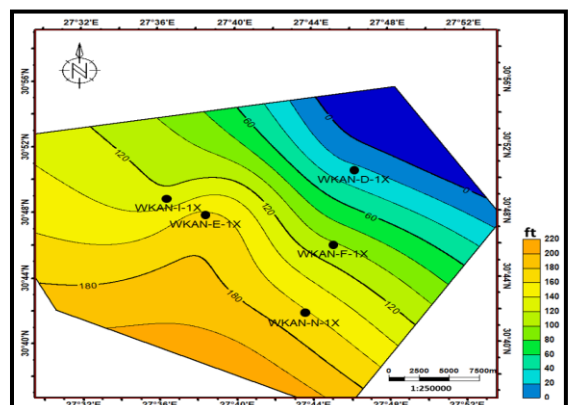


Figure 24 Limestone isolith map of the Lower Safa reservoir.

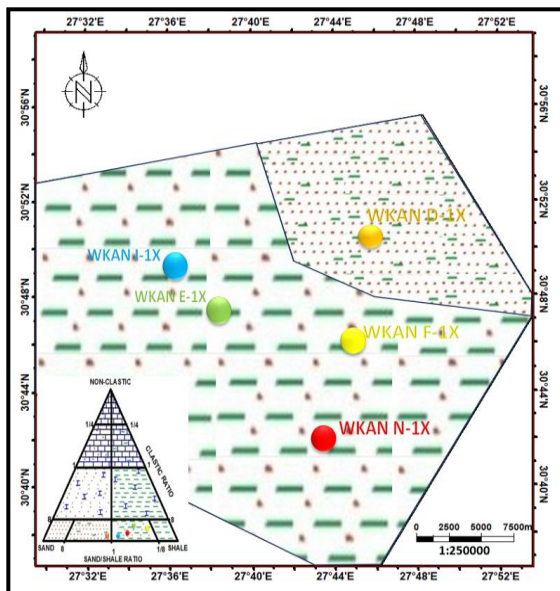


Figure 25 Triangle facies map of the Lower Safa reservoir.

Conclusions

The Lower Safa Litho-Saturation Crossplots of the wells show that the sandstone, shale, siltstone, and a few limestone and coal streaks constitute the lithology of these members.

The total thickness map of the Lower Safa Reservoir illustrated that, the rises in total thickness at west and southwest directions of the study area, with maximum value 1643 feet in WKAN I-1X well and declines towards the northeast direction of the study area, with minimum value 296 feet in WKAN D-1X well.

The total porosity map of the Lower Safa Reservoir shows the increase in the total porosity toward south part direction of the research area and gradually decreases from the middle part to the northeast direction, with maximum value of 11.1% at WKAN N-1X well, and the minimum of 7.8% at WKAN D-1X well.

At the south direction and extend to the southwest direction, the effective porosity of Lower Safa Reservoir rises, reaching 10.3% at WKAN N-1X well. Moreover, it declines toward the east direction to reach 7.3% at WKAN F-1X well.

The water saturation in the Lower Safa Reservoir increases toward the east direction and extend to the southeast direction, with maximum value of 40.3% in WKAN F-1X well, and decreases in the central part of the area, with minimum value of 15% at WKAN E-1X.

The shale volume in the Lower Safa reservoir increases toward the east direction with highest value of 17.1% in WKAN F-1X well, and decreases in the western portion of the area, with lowest value of 3.5% in WKAN I-1X well.

The net pay in the Lower Safa Reservoir increases almost in the western portion of the research area and extends to southwest directions with highest value 58 feet in WKAN I-1X well and decrease from the middle portion to the northeast directions of the research area, with lowest value 3 feet in WKAN E-1X well.

The hydrocarbon saturation map in the Lower Safa Reservoir increases at the middle portion of the area with highest value of 85% at WKAN E-1X well and

decreases laterally toward the eastern portion of the study area, with lowest value 59.7% in WKAN F-1X well.

The triangular facies map represents sandy shale facies throughout the wells region under study, as indicated by the Lower Safa Facies distribution map. These facies describe the environment as fluvio-deltaic.

Overall, the Lower Safa Reservoir's properties are getting better towards the west, south and southwest directions. The increasing levels of hydrocarbon saturation, effective porosity, and total porosity demonstrated this. In addition to rising in the same directions for net pay values.

In summary, the results indicate that the studied area has a significant quantity of hydrocarbon accumulation and presents excellent potential to drill more development and exploratory wells to increase the area productivity.

Funding sources

"This research received no external funding"

Conflicts of interest

"There are no conflicts to declare".

Acknowledgements

The authors submit deep thanks for the Egyptian General Petroleum Corporation (EGPC) for their permission to use these data to achieve this work. We are grateful to Khalda Petroleum Company (KPC) for the materials of this paper. Also, thanks are due to the Schlumberger Company for supplying us with the Interactive Petrophysics (IP, v4.3) software used in this work. Finally, deep thanks for the respected editor and reviewers for their careful reviewing of this paper.

REFERENCES

- [1] Abdullah, E. A., Al-Areeq, N. M., Al-Masgari, A., Barakat, M. Kh., 2021a. Petrophysical evaluation of the Upper Qishn clastic reservoir in Sharyoof oil Field, Sayun-Masilah Basin, Yemen. *ARNP Journal of Engineering and Applied Sciences*, 16(22); pp. 2375-2394.
- [2] Attiya, A. S., Kassab, M. A., Salem, T. M., and Abbas, A. E., 2022. Source rock evaluation and burial history modeling of the Middle Jurassic Khatatba Formation in the West Kanayes Concession of Matruh Basin, North Western Desert, Egypt, *EJCHEM*, vol 66, No. 4, pp. 71-85.
- [3] Archie, C.E., 1942: The electrical resistivity logs as an aid in determining some reservoir characteristics; *Trans; AIME*, 146: 54-62.
- [4] Asquith, G.B., 1982: *Basic well log analysis for geologists*. Published by AAPG. pp. 28-91.
- [5] Assal, E. M., El Sayed, I. S., and Hedaihed, S. M., 2021: Facies analysis, depositional architecture, and sequence stratigraphy of the upper Abu Roash "G" Member (Late Cenomanian), Sitra Field, Western Desert, Egypt. *Arabian Journal of Geosciences*, 14(12), 1-23.

- [6] Bruke, J.A., Campbell, R.L. and Schmidt, A.W., 1969: Litho-Porosity Crossplot. The Log Analyst (SPWLA), vol. 10, No. 6, 29 p.
- [7] Dresser Atlas. 1979: Log Interpretation Charts. Houston (Texas): Dresser Industries Inc.; p. 107.
- [8] El Gazzar, A. M., Moustafa, A. R., and Bentham, P., 2016: Structural evolution of the Abu Gharadig field area, northern Western Desert, Egypt.
- [9] Fawzy, A., Dahi, M., 1992: In Regional Geological Evaluation of the Western Desert, Egypt. The Geology of the Arab World. Cairo University, pp. 111–149.
- [10] EGPC (Egyptian General Petroleum Corporation), 1992: Western Desert, Oiland Gas Fields (A Comprehensive Overview). EGPC, Cairo, Egypt, p. 431P.
- [11] Hagra, M., El Awdan, H. and Gawdat, M., 1992: Hydrocarbon Potential of the Alam El Bueib Siliciclastics Revived the Industry. EGPC, 11th Petrol. Expl. Prod. Conf., Cairo, Vol. 2, p.144
- [12] Krumbein WC, Sloss LL. 1963. Stratigraphy and sedimentation. 2nd ed. San Francisco: W.H. Freeman and company, San Francisco; p. 660.
- [1] Metwalli, F.I., 2004: Assessment of Hydrocarbon Potentialities in MatruhShushan-Basins, Western Desert, Egypt: New constraints from Tectonic Subsidence Analysis and Seismic Stratigraphy. Geol. Surv., Egypt. vol. 27, pp. 497-522.
- [13] Kassab, M. A., Elgibaly, A., Abbas, A. E., and Mabrouk, I., 2021. Identification and distribution of hydraulic flow units of heterogeneous reservoir in Obaiyed gas field, Western Desert, Egypt: A case study, AAPG BULLETIN, vol 105, No. 12, pp. 2405-2424.
- [14] Poupon A, Clavier C, Dumanoir J, Gaymard R, Misk A. 1970: Log analysis of sand shale sequences – A systematic approach. J Pet Technol. 22:867–881
- [15] Said, R., 1962: Geology of Egypt: New york. El Sevier, Amsterdam, p. 317.
- [1] Sarhan, M.A., 2019: Seismic delineation and well logging evaluation for Albian Kharita formation, southwest Qarun (SWQ) field, Gindi Basin, Egypt. Journal of African Earth Sciences, 158, p.103544.
- [16] Schlumberger, 1995: In geology of Egypt. In: The Well Evaluation Conference. Schlumberger, Cairo, pp. 58–66.
- [17] Schlumberger, 1984: Well Evaluation Conference, Egypt, Geology of Egypt, p. 64.
- [18] Schlumberger, 1974: Log interpretation manual. Vol. II (Application). New York: Schlumberger Limited; p. 116 p.
- [19] Soliman, S.M., El Badry, O., 1980. Nature of cretaceous sedimentation in the Western Desert, Egypt.